Review of the Accuracy of Single Core Equivalent Thermal Model (SCETM) for Offshore Wind Farm (OWF) Cables

D. Chatzipetros, J. A. Pilgrim, *Senior Member, IEEE*

***Abstract*—Cables intended to interconnect OWFs with the mainland are currently treated as SL-type (Separate Lead) cables by IEC 60287. A SCETM is implied, i.e. a thermal model accounting for 1-D (radial) heat transfer only. While this approach is expected to be reasonable when smaller cables are rated, the 1-D representation is less valid in larger cable sizes. This paper uses 2-D finite element models to reveal certain weak points of the representation of the thermal resistances in the existing SCETM. For constant losses, the IEC SCETM seems to underestimate the temperature by up to 8ºC. Suitable replacement formulae are proposed which could improve the accuracy of the SCETM. Finally, the issue of non-solid fillers is considered and modelling guidelines are given.**

***Index Terms*—Modelling, Thermal resistance, Power cable insulation, Power transmission, Wind farms, Submarine cables.**

I. Introduction

THE number and size of installed Offshore Wind Farms (OWFs) have grown rapidly in recent years, while even larger farms are being planned, as shown in [1]. High Voltage Alternating Current (HVAC) submarine cables constitute an essential part of these projects, being used either as array cables between the generators or as export cables to connect the OWFs with the onshore transmission grid [2].

Windfarm HVAC submarine cables are currently treated as "SL-type (Separate Lead) and armoured cables" by IEC 60287 Standard ([3], [4]) where a Single Core Equivalent Thermal Model (SCETM) is implied. Although "SA-type" (Separate Aluminium) is also referred to in IEC 60287-2-1 [4], no actual distinction is made for different screen materials (thin Copper or Aluminium foils are widely used for modern array cables). Several simplifying assumptions are used by the existing SCETM, such as the sheaths being considered isothermal. Certain components inherent to the modern cable design, such as the jacketing layer above each metallic sheath, or the extruded (profile) fillers being widely used in modern cables, are not explicitly treated in IEC 60287.

This paper identifies the weak points of the thermal model currently adopted by IEC 60287 when applied to modern export and array cables. Results obtained by Finite Element Analysis (FEA) are compared with those derived from IEC calculations. It is noteworthy that the latter can underestimate the conductor temperature, whereas standard methods are normally conservative. By analysing the parameters involved and appropriately elaborating the results obtained by the FEA, analytical formulae are suggested which can be used in the present SCETM and which significantly improve its accuracy.

The paper structure reflects the main concept of the methodology followed: starting from the SCETM currently used by the IEC Standard (Section III-A), it extends towards more realistic conditions seen in the cable (Sections III-B and III-C). Finally, the questionable issue of extruded profile fillers including air gaps is evaluated and recommendations are given on how this should be modelled.

II. Existing Rating Methods

A. SCETM adopted by IEC: Thermal resistances

IEC 60287 ([3], [4]) takes advantage of the circular geometry of most of the components involved in the three-core structure and a SCETM is suggested to represent the cable based on the assumption that all the metallic parts involved are isotherms. Hence, the thermal resistance of each circular, non-metallic layer can be represented by the following equation:

$$T_i = \frac{\rho_i}{2\pi} \cdot ln\left(1 + \frac{2t_i}{d_{\text{under}}}\right) \quad (1)$$

where ρ_i is the thermal resistivity of the i-th material (KmW^{-1}), t_i is the thickness of the i-th layer (mm) and d_{under} the diameter beneath it (mm). As (5) below shows, the index i can be 1, 2j or 3, thus applying to any circular cable layer. The thermal resistance of the fillers that are used to make the assembly of cores as round as possible, and the bedding above them, are represented by T_2 and are calculated using a geometric factor G. The relevant formula is

$$T_2 = \frac{\rho_T}{6\pi} \cdot G \quad (2)$$

This work was supported by Cablel® Hellenic Cables S.A., Viohalko Group (http://www.cablel.com/).

D. Chatzipetros and J. A. Pilgrim are with the School of Electronics and Computer Science (ECS), University of Southampton, SO17 1BJ, UK. (e-mails: dc2r15@soton.ac.uk, jp2@ecs.soton.ac.uk).

D. Chatzipetros is also with the Cablel ® Hellenic Cables S.A., Viohalko Group, Sousaki Korinthias, Greece, GR 20100 (e-mail: dchatzipetros@fulgor.vionet.gr)

where ρ_T is the thermal resistivity of the material of fillers and bedding (KmW^{-1}), while a graph for G is provided by IEC 60287-2-1 [4]. The relevant IEC curves may be seen in Fig. 4. Analytical equations are also given by [4] to fit the relevant curves, depending on the ratio of the thickness of material between sheaths and armour to the outer diameter of the sheath, denoted by [4] as variable X. Since no reference is made by [4] in terms of SL-type cables with jacketed cores, either of the two curves could be potentially applicable, depending on how the jacket is treated. Extending the isothermal assumption over the outer surface of jackets, the upper curve (i.e. that assuming touching sheaths, see Fig. 4) is used in the present paper. Therefore, the SCETM remains unchanged by just adding the T_{2j} thermal resistance, while the variable X_{touch} is shown in (3). It is noted that if the lower curve was used (i.e. that assuming non-touching sheaths, see Fig. 4), then a different definition for X should be given (that shown in (4), namely X_{non_touch}), while the thermal resistance of jacket should be incorporated in T_2. However, jackets are normally made of material with different thermal properties compared with the filler.

$$X_{touch} = \frac{t_{j\_ar}}{D_j} \tag{3}$$

$$X_{non\_touch} = \frac{t_{j\_ar} + t_j}{D_{sh}} \tag{4}$$

where t_{j_ar} is the thickness of material between the external surface of jackets and the internal surface of armour (mm), t_j is the jacket thickness (mm), D_{sh} and D_j are the outer diameters over the sheath and jacket (mm), respectively, as per Fig. 1.

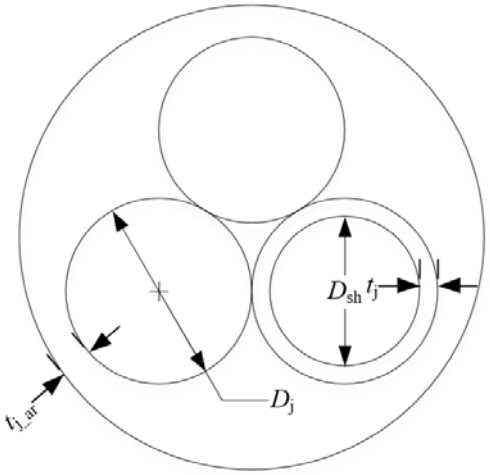

Fig. 1: A typical three-core structure where D_j, t_{j_ar} and D_{sh}, t_j are depicted.

The difference between X_{touch} and X_{non_touch} becomes even clearer from the chart shown in Fig. 2: their correlation for various t_j and for D_j ranging from 40 mm to 120 mm is depicted.

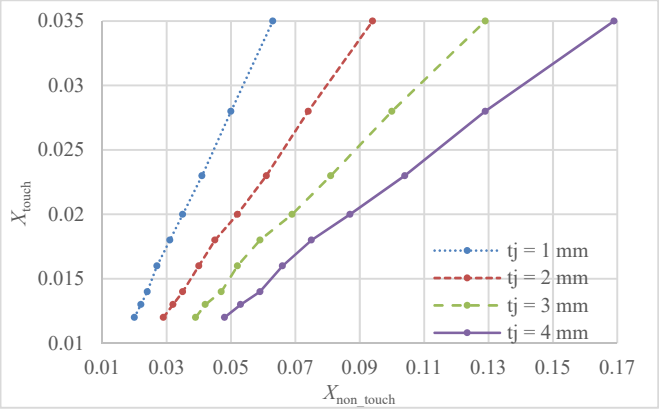

Fig. 2: Relation between X_{touch} and X_{non_touch} values.

The geometrical method used to define this factor dates back to 1923 and was developed by Wedmore [5]. Although agreement with experimental data was reported in [5], the method does impose a number of assumptions which may not be applicable to modern submarine cables.

First, Wedmore considered three core belted cables with a common Lead sheath, rather than SL-type cables with a separate sheath on each core. Furthermore, [5] uses a single thermal resistivity to represent the dielectric, including both the core insulation and filler material. Modern HVAC cables very often involve fillers with different thermal properties in comparison with core insulation, or the jacket over the sheath.

Cable geometries closer to that of SL-type have been also analysed by Anders in [6]. Screened cores are considered, while the difference between the material of fillers and that of the insulation of phase cores is addressed. However, the assumption of isothermal screen surfaces is additionally made in [6], which is questionable, as the present paper demonstrates.

The assumption of a radial thermal field implied by the existing SCETM is not fully valid in the case of SL-type cables. Owing to the close proximity between the cable cores, the principle of superposition is not applicable, since the thermal field of each core strongly affects that of the other two. One extra indication for this is that similar cable geometries are treated in a different way by IEC 60287-2-1 [4]: correction factors have been adopted for T_1, T_3 thermal resistances for three single-core cables in touching trefoil formation. Anders states that these factors are used to account for the circumferential heat conduction taking place when three cores are touching each other [7].

B. SCETM adopted by IEC: Current rating

Cables are treated as sources of heat, which must be dissipated firstly through the inherent cable components and eventually through the direct surroundings to the ambient environment. The permissible current rating is obtained by (5). The fundamental formula referred to in [3] has been appropriately modified to account for the thermal resistance of

$$I = \left[\frac{\Delta\theta - W_d[0.5T_1 + T_{2j} + n(T_2 + T_3 + T_4)]}{RT_1 + R(1+\lambda_1)T_{2j} + nR(1+\lambda_1)T_2 + nR(1+\lambda_1+\lambda_2)(T_3+T_4)}\right]^{0.5} \tag{5}$$

the jacket over each core, as implied by Anders [8]. $\Delta\theta$ is the conductor temperature rise above ambient (°C), R is the conductor ac resistance at maximum operating temperature per unit length (p.u.l.) (Ωm^{-1}), W_d is the dielectric loss p.u.l. (Wm^{-1}), T_1 is the thermal resistance between conductor and metallic sheath or screen (KmW^{-1}), T_{2j} is the thermal resistance of the jacket (KmW^{-1}), T_2 is the thermal resistance of the fillers and bedding between metallic sheath or screen and armour (KmW^{-1}), T_3 is the thermal resistance of the serving (KmW^{-1}), T_4 is the thermal resistance between cable surface and the surrounding medium (KmW^{-1}), n is the number of load carrying conductors in the cable, λ_1 is the ratio of loss in the metal sheath to the conductor loss and λ_2 is the ratio of loss in the armour to the total conductor losses.

The concept of SCETM is implemented through (5). This is investigated in the following section through FEA, first by making the same assumptions and subsequently accounting for the real conditions seen in the cable.

III. Finite Element Analysis - Methodology

A. Verification of the existing SCETM

To demonstrate the validity of Finite Element (FE) models and their comparability with the IEC Standard, the thermal model as actually considered by IEC has been developed using FEA. To consider the 1-D (radial) thermal field implied by SCETM and (5), T_2 is represented by an annulus of equivalent thickness as that depicted in (6). This formula is found just by solving (1) for t_i.

$$t_{\text{eq\_filler}} = \frac{D_j}{2} \cdot \left(e^{\frac{2\pi T_2}{\rho_T}} - 1 \right) \tag{6}$$

The armour annulus is represented as a thick layer of zero thermal resistance to keep the diameter under the serving constant, thus leaving T_3 unchanged. An indicative geometry can be seen in Fig. 3. To avoid any issues related to the depth of laying, T_4 has been set to zero, hence $\Delta\theta$ denotes the temperature rise of the conductor above the cable surface. The difference between IEC and FEA did not exceed 0.1% when identical assumptions were made.

B. Sheaths as isotherms - Verification of (2)

The aim of this part of the study is to verify (2), which is currently adopted by IEC, using the FEA. To make the two models comparable, the jackets above the phase cores are removed, meaning that the sheaths are touching. t_{j_ar} and D_j are herein replaced by t_{sh_ar} and D_{sh}, respectively, and $X_{touch} \equiv X_{non\_touch}$, while $T_4 = 0$ for the sake of simplicity. The metallic layers are assumed as isothermal by assigning extremely large thermal conductivity values to the corresponding geometrical entities. Additionally, the thermal properties of the bedding and filler regions are considered to match, as implied by IEC. Hence, the thermal resistance of the filler is obtained from the FEA as (7) indicates.

$$T_{2,\text{FEA}} = \frac{\theta_{sh} - \theta_a}{3W_c(1+\lambda_1)} \tag{7}$$

where θ_{sh}, θ_α are the temperature of the sheath and armour, respectively (°C) and W_c is the conductor loss applied (W/m). It should be noted that both $\lambda_1, \lambda_2 = 0$ during the extraction of $T_{2,FEA}$ for the sake of simplicity. Nevertheless, some indicative cases with $\lambda_1, \lambda_2 \neq 0$ confirmed what was expected, i.e. accounting for both λ_1, λ_2 has no effect in terms of $T_{2,FEA}$ value.

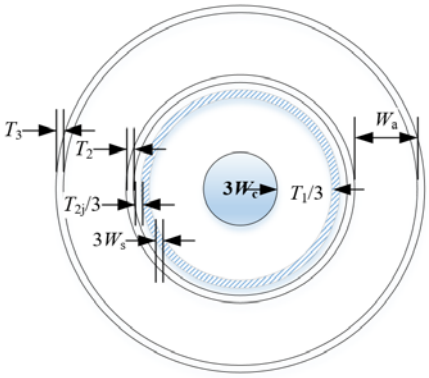

Fig. 3: An illustration of the SCETM considered by IEC including the jacket extension proposed by Anders [8].

Then, by solving (2) for G and varying X_{touch}, the curve in Fig. 4 was obtained. It should be noted that varying both t_{sh_ar} and D_{sh} do not change the FEA curve in Fig. 4, as expected. In other words, the same G value occurs whatever the combination of t_{sh_ar}, D_{sh} is, on the condition that their ratio X is kept unchanged. This may be explained by the fact that although heat encounters locally higher thermal resistance because of the increased t_{j_ar}, better heat dissipation occurs from the increased core surface (because of the increase in D_{sh}) close to the armour bedding. For comparison, Fig. 4 also shows the IEC curves.

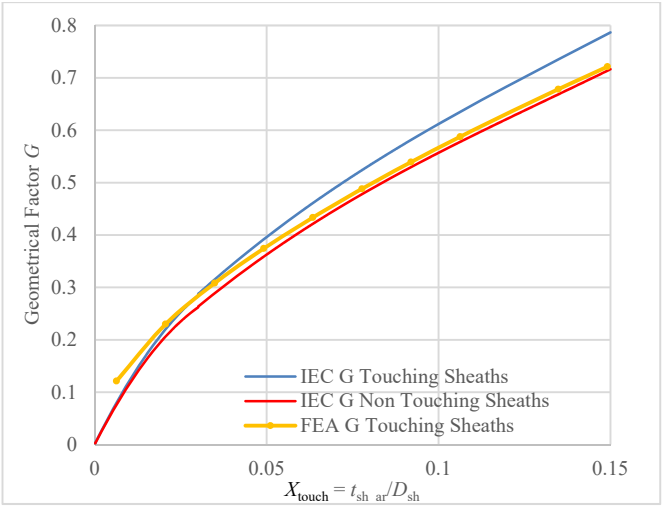

Fig. 4: G curve derived from FEA – Isothermal sheaths considering power cores with no jacket.

The G curve calculated by FEA stands between the two IEC curves, except for the extremely low X_{touch} region where slightly higher G values appear. The difference will be defined as "*geometrical error*" in the context of the present paper. This differs from the "*thermal error*" defined in Section III-C. The divergence observed in Fig. 4 may be attributed to the fact that

it is not very clear how thick the IEC method assumes the material between sheath and armour is in the case of touching sheaths. Moreover, as the geometrical method considered by Wedmore in 1923 did not have metallic sheaths on each core [5], the lines of heat-flow would have a slightly different distribution compared with those derived from an SL-type geometry. Nevertheless, the divergence noticed is not significant, with the relative difference between FEA and IEC being lower than 10% in most cases.

C. Sheaths as non-isotherms

To derive a more representative curve accounting for the more realistic 2-D heat conduction, the Lead sheaths are no longer treated as isotherms; instead, finite, typical book values are assigned in terms of the thermal conductivity of Lead. Since the temperature along the sheath circumference is not fixed, the average value has been applied to obtain an as representative as possible estimation of temperature. This is used for θ_{sh} in (7). Power cores with no jacket are again assumed, as before. The surfaces of conductors and armour are still treated as isotherms, while a Lead sheath of 2.0 mm thickness has been assumed. The relevant curve is depicted in Fig. 5 along with the IEC curves.

As may be readily noticed from Fig. 5, significant divergence occurs between FEA and IEC G values when the Lead sheaths are treated as non-isothermal. This "*thermal error*" seems to be significantly larger than the *geometrical* one: relative differences above 50% can be noticed, especially for lower X_{touch} values. It should be noted that the domain of lower X_{touch} values is quite possible in practice, since it relates to larger D_{sh} compared with t_{sh_ar}, where the latter would typically be less than 5mm but the former could reach up to 100 mm.

Furthermore, the larger FEA G values for lower X_{touch} seem to reveal another weak point of the existing SCETM: significant 2-D (circumferential) heat conduction is expected to take place due to the touching arrangement of the phase cores and consequently the non-applicability of the principle of superposition. The peripheral thermal resistance of the Lead sheath is responsible for the large divergence with IEC curves. Much lower discrepancy can be observed for higher X values, namely lower D_{sh} with respect to the Lead sheath thickness. In other words, the thicker the Lead sheath (or equally the shorter the sheath circumference) the closer to the results derived upon the isothermal assumption and thus to the IEC G curves.

In conclusion, the *geometrical error* should not be treated regardless of the *thermal* one, since the latter appears to be more severe. This paper suggests the simultaneous treatment of both *errors*. The following section shows the process followed to approach this issue through FEA, then subsequently using analytical equations.

IV. Suggested Correction Of The Existing IEC Thermal Model

An indication about the divergences introduced by the existing SCETM and their mitigation via G factor has been obtained from Section III. A new formulation is proposed which is easily adoptable by the existing SCETM and expected to improve its accuracy. The circumferential thermal resistance of the metallic sheath is of great importance, as shown in Section III.

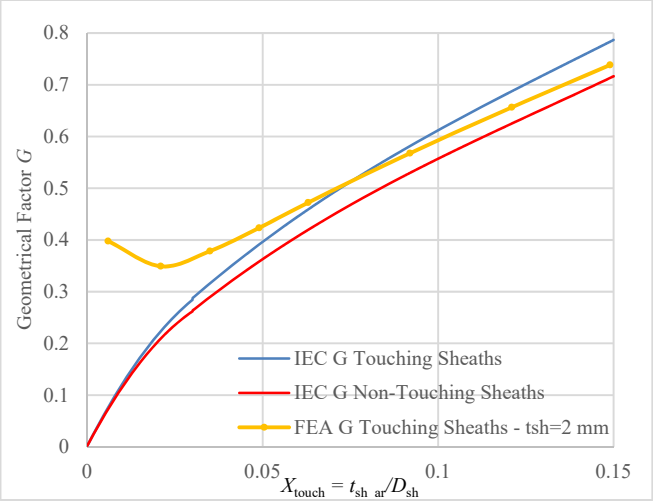

Fig. 5: G curve derived from FEA – Non-isothermal sheaths considering power cores with no jacket.

The lead sheath of a typical OWF export cable falls within the range 2 – 5 mm. On the contrary, typical array cables very often comprise Copper (Cu) or Aluminium (Al) laminated tapes of thickness 0.15 – 0.3 mm as metallic screening. Our analysis explicitly considers jacketed cores, as typically used in modern OWF cables. Hence, the average temperature above the outer surface of the jackets, namely θ_j, instead of metallic sheaths is obtained from FEA. This has replaced the value of θ_{sh} in (7), while the surfaces of both the conductors and armour are still treated as isotherms.

A. Proposed G curve for SL-type cables

Several G curves have been derived by varying X and the thickness of Lead sheath. To simplify the analysis, a jacket thickness (t_j) equal to 1 mm, as well as a thickness between jacket and armour (t_{j_ar}) equal to 2 mm have been considered for all the cases. The impact of making these assumptions is separately considered in Section IV-B.

For each thickness, the value of D_j has been varied every 10 mm in the range 32 - 152 mm to obtain an as accurate and representative as possible fitted curve. Values of D_j out of this range are not expected for the vast majority of OWF cables. Linear fitted curves are proposed, as illustrated in Fig. 6. The two G curves as considered by IEC are shown in the same chart, while focus has been made on the area of interest.

Although not perfect, the linear approximation affords the necessary simplicity to proceed with the analysis. Besides, most of the lines seem to fit the relevant points accurately enough, except for that of 1 mm thickness. Testing higher D_j values, while at the same moment keeping a very thin metallic sheath, the FE model geometry becomes more extreme and numerical errors are more likely to occur owing to the correspondingly poor density of mesh. All the G curves extracted by FEA are above those by IEC, thus implying that the existing SCETM represents the filler in a more optimistic way, because of treating the metallic sheaths as isotherms. The proposed curves for

thicker sheaths are closer to the IEC values, since the circumferential thermal resistance of the Lead sheath decreases and it becomes more isothermal.

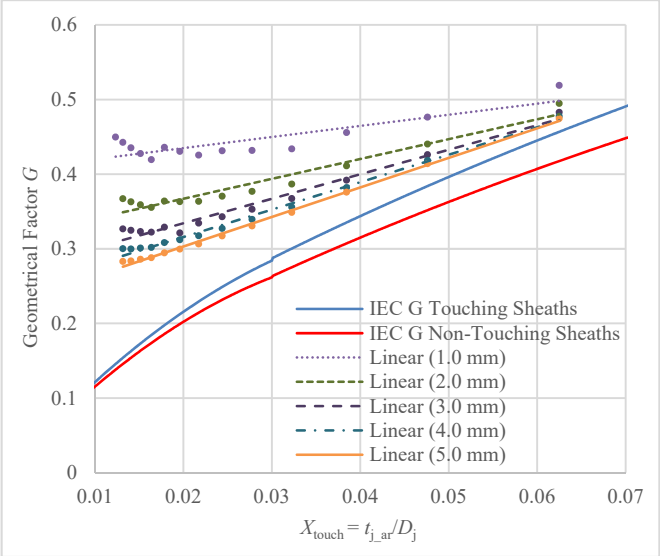

Fig. 6: Derivation of G curves against thickness of sheath.

Having the a and b terms of each line, namely $G = a \cdot X_{touch} + b$, polynomial relations of 3rd order have been used to match the corresponding (a, t_s), (b, t_s) points, where t_s is the thickness of the sheath. The following formula correlating both t_s and X_{touch} variables was found:

$$G(X_{touch}, t_s) = (a_3 \cdot t_s^3 + a_2 \cdot t_s^2 + a_1 \cdot t_s + a_0) \cdot X_{touch} + (b_3 \cdot t_s^3 + b_2 \cdot t_s^2 + b_1 \cdot t_s + b_0) \quad (8)$$

where $a_3 = 0.0368$, $a_2 = -0.4749$, $a_1 = 2.3253$, $a_0 = -0.3956$, $b_3 = -0.0032$, $b_2 = 0.0404$, $b_1 = -0.189$, $b_0 = 0.5567$.

B. Review of the assumptions made

As mentioned in Section IV-A, fixed values of t_j and t_{j_ar} were used for the derivation of (8) for the sake of simplicity. In terms of the former (t_j), jacketing layers have a much lower (about two orders of magnitude) thermal conductivity than the Lead sheaths, thus preventing large amounts of heat from dissipating through them. To check for any likely effect t_j has on the G curves obtained, values up to $t_j = 4$ mm were examined and the relative difference with FEA did not exceed 10%. This compares to divergences of up to 55% between FEA and the existing IEC G. Although the assumption of 2 mm for t_{j_ar} is arbitrary, it is representative of the typical thickness of a single layer of yarn bedding. Beddings of up to $t_{j\_ar} = 4$ mm were tested, resulting in a difference between FEA and the proposed curves not exceeding 8%, while at the same moment the respective IEC figure was 30%, thus confirming that the proposed curve remains more accurate with respect to FEA. The results of these checks are shown in Fig. 7 and Fig. 8 where the indicative case of $t_s = 2$ mm has been considered (similar results have been derived for various t_s).

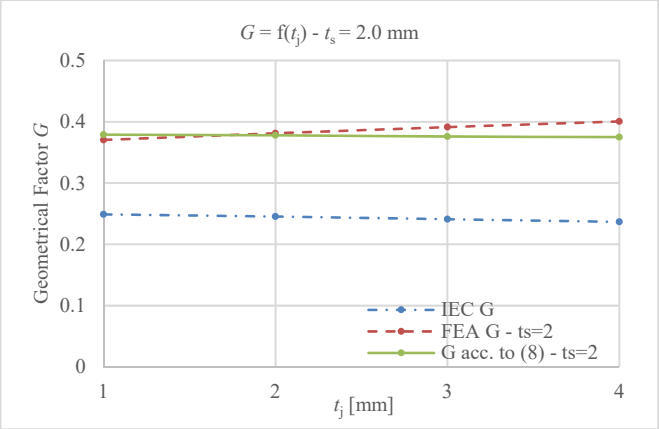

Fig. 7: G curve derived from (8) against those extracted by FEA and suggested by IEC for various t_j values keeping t_{j_ar} = const. = 2.0 mm.

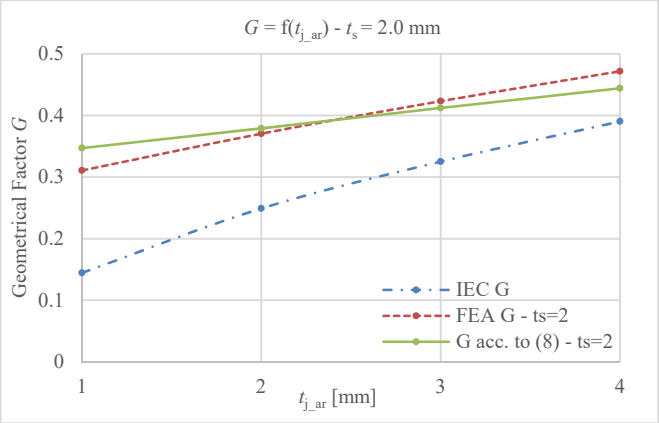

Fig. 8: G curve derived from (8) against those extracted by FEA and suggested by IEC for various t_{j_ar} values keeping t_j = const. = 1 mm (or equally D_j = const. = 82 mm).

C. Proposed G curve for metallic foil screened cables

Wind farm array cables are often screened by Cu or Al laminated tapes to reduce their weight and cost. Applying the same methodology as presented in Section IV-A, new G curves are found for foil screened cables. The foil thickness is expected to vary much less compared with the SL-type case, typically in the range 0.15 - 0.3 mm. A foil of 0.2 mm has been assumed in terms of the relevant curves. The latter can be seen in Fig. 9, along with the extreme curves of SL-type for comparison. D_j was considered to vary in the range 30 - 80 mm, since array cables have smaller conductor size and insulation thickness.

The foil curves stand between those with 1.0 mm and 5.0 mm Lead thickness, with that of Cu being closer to the IEC curves. This may be attributed to the higher thermal conductivity of Cu in comparison with Lead, in spite of the much smaller thickness of the metallic foil. In other words, the better conductivity of Cu (almost one order of magnitude higher than Lead) makes the relevant curve closer to the isothermal one, whereas the slightly worse conductivity of Al (almost half of Cu) results in higher G values.

Having assumed constant thickness for the metallic foil, an equation depending only on X_{touch} can be found. The relevant formulae for Copper and Aluminium are shown in (9) and (10), respectively.

$$G(X_{\text{touch}})_{Cu} = 3.5164 \cdot X_{\text{touch}} + 0.2819 \quad (9)$$

$$G(X_{\text{touch}})_{Al} = 2.9422 \cdot X_{\text{touch}} + 0.3317 \quad (10)$$

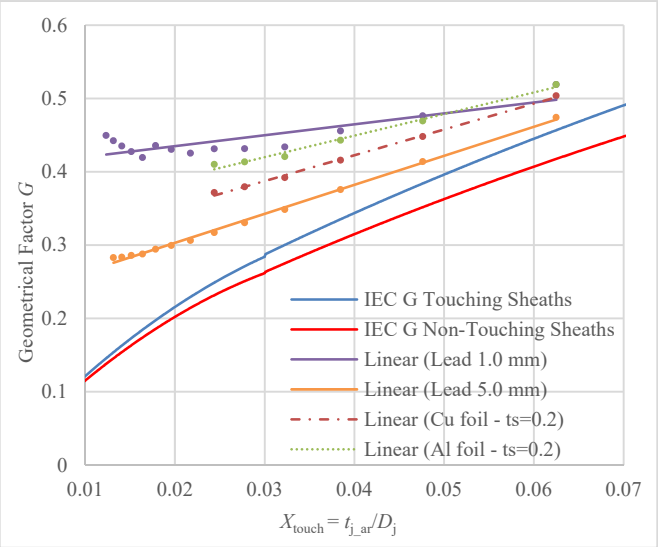

Fig. 9: Derivation of G curves against material of metallic foil.

V. Effect on Cable Temperature

New curves for the geometric factor have been suggested in Section IV to represent in a more realistic way the thermal resistance of fillers T_2, and improve the accuracy of the existing SCETM. As shown in Fig. 6 and Fig. 9, the G values extracted by FEA tend quite close to those suggested by IEC for large X_{touch} values. Nevertheless, by decreasing X_{touch} much higher discrepancies are noticed, especially if this reduction is due to increased D_j and simultaneously reduced t_s. An extreme difference of about 200% was observed for the thinnest Lead sheath. This is of particular importance, since it implies that the existing IEC Standard represents smaller OWF cables sufficiently, but not larger export cable sizes. This could be also justified by the fact that an SL-type cable with a relatively high X_{touch} (i.e. thick bedding or equally small core diameter) looks closer to the cable geometry treated by Wedmore [5].

In order to check for the applicability of (8)-(10) and the degree of improvement, FE models of buried submarine cables are compared with the existing SCETM. It should be noted that the filler is assumed to be of the same material as the armour bedding for the sake of simplicity. Although this is not always the case, the armour bedding mostly consists of Polypropylene (PP) yarns, while PP ropes are often used as a filler material in OWF cables. Finally, the issue of extruded (profile) fillers is reviewed, making focus on the extent to which they could be treated as though they were solid.

A. FE Models – Assumptions made

FE models have been used by many researchers [9] for the rating of cables and are potentially more representative and accurate than the conventional IEC analytical methods ([3], [4]). This paper considers a de-coupled steady-state thermal response of the cable accounting for the IEC thermal losses prescribed by [3]. The IEC armour loss has been chosen despite recent publications ([10], [11]) indicating that this might be an over estimation of the thermal armour loss, since the present paper deals only with the thermal resistances.

Following a similar approach as suggested by Swaffield [9], the semi-infinite soil was represented by a rectangle with both vertical boundaries being treated as adiabatic (no heat flux passes through them), while the bottom temperature was assigned a value of 12°C to represent the remote ground temperature. The latter seems to vary between 10 and 16°C according to [12], while the value of 12°C is also suggested by [13]. Similar treatment in terms of 2-D FEA for cables has been proposed by other researchers, such as Kocar [14] and Catmull [15]. The cable is buried 1 m from the seabed surface, the soil thermal resistivity is assumed $\rho = 0.7$ KmW^{-1}, while an isotherm of 15°C is applied on the seabed surface. Finally, concerning the modelling of the cable itself, the semiconductive layers over and below the main insulation of each core have been considered to be of the same thermal resistivity as that of the insulation to make IEC and FE models as comparable as possible, since the former assumes a single, uniform thermal layer.

B. Solid fillers

The results derived by both calculation tools are illustrated in Table I. Three different lead sheath thicknesses are tested, while cables at 66 kV, 150 kV and 220 kV with various cross-sectional areas (XSAs) have been modelled. Neither the voltage level nor the selection of XSA are expected to have any significant effect on the results. However, by varying the XSA and rated voltage, X_{touch} is expected to accordingly change due to the varying conductor diameter and insulation thickness. Hence, D_j varies from 43 mm up to about 122 mm, keeping t_{j_ar} = const. = 1.4 mm. Thus, the wider applicability of the proposed G formula can be checked.

To make the comparison clearer, the ampacity was initially calculated through IEC assuming 90°C as the maximum permissible temperature. The same current was then applied into the FE model and the temperature obtained was recorded. The difference between these two values is noted in Table I as *Initial Difference*, taking the FEA value as a reference. Subsequently, the G formula as described by (8) was used and the elevated IEC temperature was recorded. The difference between the modified IEC and FEA was again recorded and is noted as *Final Difference* in Table I, taking the FEA value as a reference. The results shown in Table I clearly imply that the present SCETM underestimates the temperature, in some cases by about 7-8°C. In particular, the thinner the Lead sheath and simultaneously the larger its circumference (thus decreasing X_{touch}), the higher the divergence reported in relation to the FEA results.

As it is shown, better agreement between the values derived by the modified SCETM and the FEA can be noticed in most of the cases. An exception may be observed in the last case, where the *Final Difference* seems to be larger in absolute values than the *Initial* one. However, this case represents a rather non-typical cable design: small OWF cables (thus increasing X_{touch}) do not generally have a thick Lead sheath. On the contrary, thicker sheaths are not unusual in larger export cables. It is also

noteworthy that the existing SCETM seems optimistic for modern cables, whereas the suggested modification appears to yield results on the safe side. This is clearly implied by the negative sign of the values being in the *Initial Difference* column, while positive values are depicted in the *Final Difference*.

TABLE I
COMPARISON OF RESULTS OBTAINED BY FEA & MODIFIED SCETM – SL-TYPE CABLES

X_{touch} (t_{j_ar}/D_j)	Lead sheath thickness, t_s [mm]	FEA [°C]	Modified SCETM [°C]	Initial Difference [°C]	Final Difference [°C]
0.012 (1.4/122)	1.5	97.7	98.8	-7.7	1.1
	2.5	96.6	97.1	-6.6	0.5
	3.5	95.5	96.3	-5.5	0.8
0.016 (1.4/88)	1.5	96.9	97.6	-6.9	0.7
	2.5	95.8	95.8	-5.8	0.0
	3.5	94.4	95.0	-4.4	0.6
0.033 (1.4/43)	1.5	93.6	94.7	-3.6	1.1
	2.5	91.9	93.3	-1.9	1.3
	3.5	91.0	92.6	-1.0	1.6

Similarly good agreement between the modified SCETM and FEA has been also obtained for the case of metallic foil screened cables. To derive the temperature values with respect to the modified SCETM, (9) and (10) have been used, while a thickness of 0.2 mm was assumed in any case. Although this parameter slightly varies in reality (not more than ±0.1 mm), its effect on the accuracy is not significant if the same equations are applied. Following the same procedure as for the SL-type case, three X_{touch} values were examined, keeping t_{j_ar} = const. = 1.2 mm and varying D_j from 42 mm up to 65 mm. The relevant results can be seen in Table II.

TABLE II
COMPARISON OF RESULTS OBTAINED BY FEA & MODIFIED SCETM – METALLIC FOIL SCREENED CABLES

X_{touch} (t_{j_ar}/D_j)	Foil Material	FEA [°C]	Modified SCETM [°C]	Initial Difference [°C]	Final Difference [°C]
0.019 (1.2/65)	Al	95.9	96.5	-5.9	0.6
	Cu	95.2	95.2	-5.2	0.0
0.023 (1.2/53)	Al	95.6	95.3	-5.6	-0.3
	Cu	95.1	94.1	-5.1	-1.0
0.029 (1.2/42)	Al	95.6	95.4	-5.6	-0.2
	Cu	94.9	94.1	-4.9	-0.8

C. Extruded (Profile) fillers

Extruded (profile) fillers are very often used instead of solid ones in OWF cables to give the assembly of cores a more round geometry. Unlike the solid fillers made by PP ropes, they typically comprise gaps to make the cable less stiff and at the same moment to enclose other composite elements, e.g. optical cable units. An indicative geometry is shown in Fig. 10. Although the gaps are expected to be filled with water in subsea sections of the cable route, air-filled gaps can occur at the J-Tubes or the landfall sections where the cable interstices may not be saturated. Hence, the representation of these fillers by the existing SCETM is rather questionable.

Owing to the poor thermal conductivity of air, very conservative results would occur if only conductive heat transfer were taken into account, although this may be valid where the cable is installed in water. On the other hand, convective heat transfer may not be assumed owing to the small size of the gaps and the low temperature gradient across them. However, radiative heat transfer could be a quite realistic assumption when air fills the gaps.

The heat flow rate of radiation exchange between two surfaces i, j is given by (11) [7]:

$$Q = \varepsilon \cdot \sigma_B \cdot A_{sr} \cdot \left(\theta_i^4 - \theta_j^4\right) \tag{11}$$

where ε is the emissivity of the surface, σ_B is the *Stephan-Boltzmann* constant ($5.67 \cdot 10^{-8}$ W/m^2·K^4), A_{sr} is the effective radiation area (m^2) and θ_i, θ_j is the temperature of the i-th and j-th surface, respectively (°C).

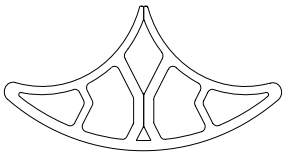

Fig. 10: Indicative extruded (profile) filler geometry.

It is difficult to precisely define the surface emissivity, as it is strongly material dependent. Anders [7] refers 0.9 for PVC and PE materials which are often used for profile fillers, though without mentioning any variation around colour or finish. The same values are also cited by EPRI authors in [16]. The filler geometry is expected to affect the results obtained, since the contribution of each heat transfer mode, namely conduction and radiation, varies depending on the size of the gaps. Both parameters are herein examined and analysed through FEA.

For the sake of simplicity, a filler geometry very close to that illustrated by Fig. 10 was initially modelled; circular disks have replaced the irregular shapes representing the gaps. Then, the geometry was further simplified, though keeping the same ratio between the gap region and the solid material. Both geometries are illustrated in Fig. 11. A relative difference of maximum 0.5% in terms of conductor temperature occurred between the two geometries by varying ε. Hence, the simplified geometry may be considered accurate enough and this is subsequently used, since it is easier to handle.

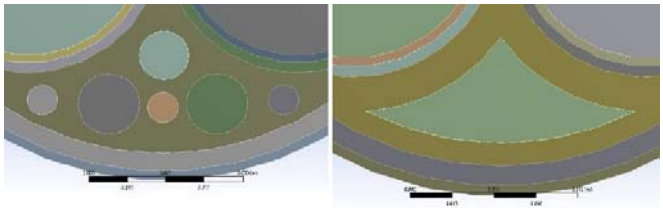

Fig. 11: Actual and simplified filler geometries.

Three different geometries were examined through FEA, varying each time the ratio of the gap area in relation to that of solid material. The gap is considered being filled with still air (no convection), while the emissivity varied from 0.5 to 1.0. At the same time, models accounting for totally solid fillers were assumed, i.e. replacing the air in the gap by the material of the filler, while the heat source was kept constant in all cases. The relevant results are depicted in Fig. 12.

As it can be seen from the results, the temperature rise depends more on the emissivity of filler material as the air gap section increases and the heat transfer is more dominated by the conduction through air. If the assumption of $\varepsilon = 0.9$ is considered, a divergence of about 0.8% exists between the solid and the realistic filler with gaps, thus keeping the geometry of minor importance. If a more conservative assumption is made, for instance that of $\varepsilon = 0.5$, a difference of 2% is reported in terms of the extreme geometry of 74% air gap and 26% solid material. In this case the geometry plays an important role. In conclusion, the extruded (profile) fillers could be treated as though they were solid, depending on the assumption made about ε and the geometry considered. Since ε is not that easy to define, a structure with more solid material constitutes a safer assumption and hence (8)-(10) of the present paper can be used for calculating T_2 in analytical calculations.

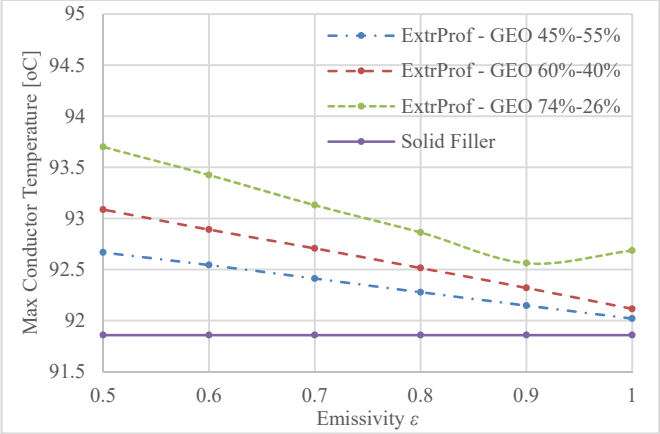

Fig. 12: Temperature results for different filler geometries considering various emissivity values. In each case the area of the air gap followed by that of solid filler are noted.

VI. Conclusions

The work presented in this paper identifies certain weak points of the existing SCETM adopted by IEC 60287 when rating OWF cables. The current Standard method does not account for the thermal impact of different screen materials and the 1-D thermal representation is not always valid.

The FE models show a good agreement with the existing Standard method when the metallic sheaths are treated as isotherms. Additionally, relatively small divergences are noticed when small core sizes are modelled. However, significant discrepancies with the existing SCETM are observed for larger core sizes, especially when the corresponding sheath thickness is small. This is particularly important for the forthcoming OWF projects which are expected to include increasingly larger cable sizes, as the results present here show that the SCETM model can underestimate the temperature by up to 8ºC.

New analytical formulae for the geometric factor G applicable to all modern OWF cable sizes are suggested to improve the accuracy of the present SCETM, as verified through comparison to a finite element model. As shown, they reduce the divergence between SCETM and FEA from 8ºC by means of the existing IEC Standard up to 1ºC by means of the proposed formulae, additionally being on the safe side when tested for typical subsea installation conditions. Although experimental validation would be valuable, the difficulty in measuring the non-isothermal nature of the sheath and bedding layers are likely to lead to additional measurement error. As the thermal conduction can be modelled to a high accuracy using FEA, a high level of confidence can be held in the modelled results.

Finally, the increasingly used extruded (profile) fillers can be in some cases considered as solid, particularly if the filler material prevails against the gap area.

VII. Acknowledgment

Mr. Chatzipetros gratefully acknowledges the contribution of his colleague and friend Dr. Andreas I. Chrysochos for his comments and suggestions in preparing this paper.

VIII. References

[1] Andrew Ho, Ariola Mbistrova (2017, January). The European offshore wind industry: Key trends and statistics 2016. WindEurope Business Intelligence. Brussels, Belgium. [Online]. Available: https://windeurope.org/wp-content/uploads/files/about-wind/statistics/WindEurope-Annual-Offshore-Statistics-2016.pdf

[2] CIGRE, “Offshore Generation Cable Connections.”, Technical Brochure 610, Working Group B1.40, February 2015

[3] IEC 60287, “Electric cables - calculation of the current rating - part 1-1: Current rating equations (100% load factor) and calculation of losses - general.”, Technical report, International Electrotechnical Commission, 2014-11.

[4] IEC 60287, “Electric cables - calculation of the current rating - part 2-1: Thermal resistance - Calculation of thermal resistance.”, Technical report, International Electrotechnical Commission, 2015-04.

[5] S. W. Melsom, “Permissible Current Loading of British Standard Impregnated Paper Insulated Electric Cables, Second Report on the Research on the Heating of Buried Cables”, Appendix IV: “Calculation of the Thermal Resistance of Three-Core Cables and Examination of Russell’s Formula”, IEE, Vol. 61, No. 318, May 1923.

[6] G. J. Anders, A. Napieralski, Z. Kulesza, “Calculation of the Internal Thermal Resistance and Ampacity of 3-Core Screened Cables with Fillers”, IEEE Transactions on Power Delivery, Vol. 14, No. 3, July 1999.

[7] G. J. Anders, “Rating of Electric Power Cables – Ampacity Computations for Transmission, Distribution and Industrial Applications”. IEEE Press series on Power Engineering, 1997.

[8] G. J. Anders, George Georgallis, “Transient analysis of 3-core SL-type submarine cables with jacket around its core.”, In Jicable ’15, Versailles, France, 2015

[9] D. J. Swaffield, P. L. Lewin, S. J. Sutton, “Methods for rating directly buried high voltage cable circuits”, IET Generation, Transmission & Distribution, September 2007.

[10] J. J. Bremnes, G. Evenset, R. Stølan. “Power Loss And Inductance Of Steel Armoured Multi-Core Cables: Comparison Of IEC Values With “2,5D” FEA Results And Measurements.” B1-116, CIGRE 2010.

[11] Kevin F. Goddard, James A. Pilgrim, Richard Chippendale, and Paul L. Lewin. “Induced Losses in Three-Core SL-Type High-Voltage Cables.” IEEE Transactions on Power Delivery, Vol. 30, No. 3, June 2015.

[12] British Geological Survey, Natural Environment Research Council, GeoReports, BGS Report No. GR_999999/1. (2011, May). Temperature

and Thermal Properties (Detailed). UK. [Online]. Available: https://shop.bgs.ac.uk/GeoReports/examples/modules/C011.pdf
[13] P. L. Lewin, J. E. Theed, A. E. Davies, and S. T. Larsen. Methods for rating power cables buried in surface troughs. IEE Proceedings: Generation, Transmission and Distribution, 146(4):360–364, July 1999.
[14] I. Kocar, A. Ertas. Thermal Analysis for Determination of Current Carrying Capacity of PE and XLPE Insulated Power Cables Using Finite Element Method. IEEE Melecon, Dubrovnik, Croatia, May 2004.
[15] Simon Catmull, Richard D. Chippendale and James A. Pilgrim. Cyclic Load Profiles for Offshore Wind Farm Cable Rating. IEEE Transactions on Power Delivery, Vol. 31, No 3, June 2016.
[16] S. Eckroad, "EPRI Underground Transmission Systems Reference Book". Electric Power Research Institute (EPRI), Palo Alto, CA: 2006. 1014653.

IX. BIOGRAPHIES

Dimitrios Chatzipetros received the Dipl. Eng. degree from the School of Electrical and Computer Engineering at the National Technical University of Athens, Greece, in 2012. His research interests include modelling aspects of High Voltage equipment, such as Field Analysis for Insulators and Thermal Analysis for Cables.

He works as a Cable Design Engineer in Cablel® Hellenic Cables S.A., Viohalko Group. He is currently pursuing the Ph.D. degree in Electrical Power Engineering at the University of Southampton, Southampton, U.K. His Ph.D. project is concerned with the optimisation of submarine cables intended to interconnect OWFs with the mainland.

James A. Pilgrim (M'09, SM'17) received the Bachelor's degree in electrical engineering from the School of Electronics and Computer Science at the University of Southampton in 2007. He joined the staff of the University of Southampton in 2007 as a Research Assistant, gaining his PhD in 2011. He joined the academic staff of the University in 2012. His research interests include all aspects of high voltage cables and associated insulation systems. He is currently the Treasurer of the UKRI Chapter of the IEEE DEIS and Chair of the DEIS Technical Committee on Smart Grid. He is actively involved in the development of current rating methodologies, acting as the UK member of IEC TC 20 WG19 (Current Rating and Short Circuit Limits of Cables) and Cigre Working Groups B1.35 "Guide to rating calculations" and B1.56 "Current rating verification".